LIQUID EXTRUSION TECHNIQUES FOR PORE STRUCTURE EVALUATION OF NONWOVENS

Akshaya Jena and Krishna Gupta
Porous Materials, Inc., 83 Brown Road, Ithaca, NY 14850

ABSTRACT

Two variations of the liquid extrusion technique for pore structure analysis have been analyzed and results obtained using nonwoven materials have been discussed. Strengths and limitations of the techniques have been evaluated. The techniques can measure all the important pore characteristics of nonwovens without using any toxic material or high pressures.

1. INTRODUCTION

Pore structure characteristics of nonwovens are important for their applications. Three kinds of pores may be present in a material (Figure 1). The closed pores are not accessible. The blind pores terminate inside the material and do not permit fluid flow. The through pores are open to the outside and permit fluid flow. Through pores are of primary interest for many of the applications of nonwovens. The important through pore characteristics of nonwovens include the most constricted pore diameters, the largest pore diameter, the mean pore diameter, pore volume, pore distribution, surface area, gas permeability and liquid permeability.
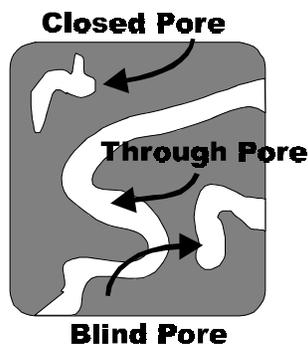

Figure 1. Three kinds of pores.

Mercury intrusion porosimetry is often used to characterize the pore structure of nonwovens. In this technique mercury is forced into pores under pressure and intrusion volume and pressure are measured. However, this technique detects only the pore volume and diameters of through and blind pores. None of the other important characteristics are measurable. Also, mercury intrusion requires very high pressures, which may significantly distort the pore structures of nonwovens. Mercury used in this technique is harmful to one's health and pollutes the environment. In contrast, the liquid extrusion techniques have a number of advantages. In these techniques, a wetting liquid fills the pores of the sample and a pressurized gas extrudes the liquid from pores. Pressure and gas flow rate or extruded volumes of liquid are measured. The extrusion techniques can determine all the important pore characteristics. No toxic material is used. The pressure required is an order of magnitude less than that required for mercury intrusion so that distortion of pore structure due to pressure is insignificant. The liquid extrusion techniques, their strengths and limitations have been discussed and results obtained using these techniques have been critically examined. Mercury intrusion technique is briefly considered for comparison.

2. TECHNIQUES

2.1 Liquid Extrusion Technique

Principle: A liquid, whose surface free energy with the sample is lower than that of the sample with gas is used to fill the pores of the sample. Because of the reduction in the free energy of the system the pores are filled spontaneously. A non-reacting gas is employed to force the liquid out of the pores. The gas can displace the liquid in a pore, provided work done by gas is equal to the increase in surface free energy required for the replacement of the low free energy sample-liquid surface by the high free energy sample –gas surface (Figure 2) [1].

$$p \, dV = (\gamma_{s/g} - \gamma_{s/l}) \, dS \tag{1}$$

where p is differential pressure, dV is displaced volume of liquid in the pore, $\gamma_{s/g}$ is solid-gas surface free energy, $\gamma_{s/l}$ is solid-liquid surface free energy and dS is increase in solid-gas surface area (decrease in solid-liquid surface area). The change in the liquid-gas inter-facial area is usually negligible [2].
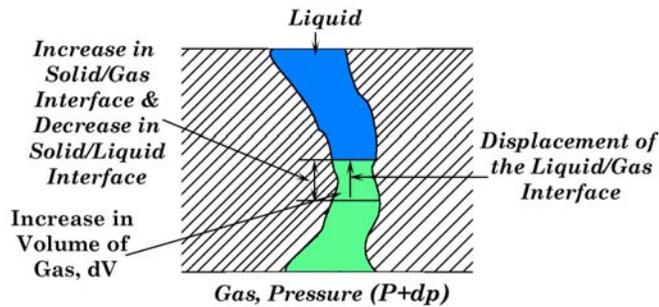

Figure 2: Displacement of wetting liquid in a pore.

Consideration of equilibrium between surface tensions (Figure 3) leads to [3]:

$$(\gamma_{s/g} - \gamma_{s/l}) = \gamma \cos \theta \tag{2}$$

where γ is the surface tension and θ is the contact angle of the wetting liquid. From Equations 1 and 2:

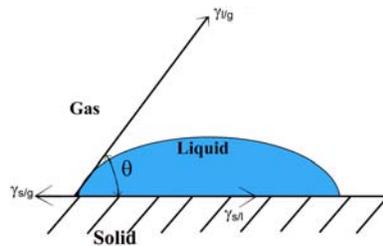$$p = \gamma \cos \theta \, (dS/dV) \tag{3}$$

Figure 3. Equilibrium between surface tensions.

Definition of pore diameter: Pore surfaces normally converge and diverge in irregular manner creating irregular pore cross-sections along pore path. Consequently, a pore cross-section may not be associated with a well defined pore diameter. A few examples are illustrated in Figure 4.

Figure 4. Pore cross-sections.

The pore diameter, D, is defined such that:

$$(dS/dV)_{pore} = (dS/dV)_{circular\ opening\ of\ diameter,\ D} = 4/D \qquad (4)$$

From Equations 3 and 4:

$$p = 4\ \gamma \cos\theta / D \qquad (5)$$

Equation 5 suggests that increasing gas pressure removes liquid from decreasing pore diameter. The liquid extrusion techniques measure differential gas pressure, gas flow rates through emptied pores or volume of extruded liquid. Many pore structure characteristics are computed from these measured quantities.

2.2 Capillary Flow porometry

Capillary flow porometry is a liquid extrusion technique in which the differential gas pressure and flow rates through wet and dry samples are measured (Figure 5) [4]. Pore diameters, the largest pore diameter, the mean flow pore diameter, pore distribution, envelope surface area (through pore surface area) and gas permeability are computed. Liquid permeability is also measurable in this technique.
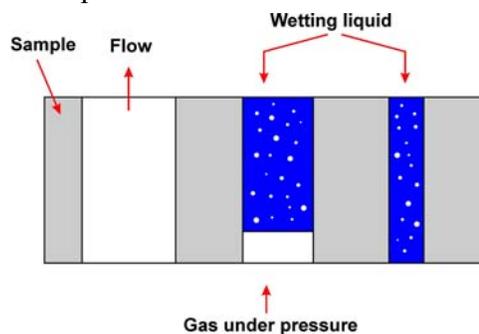

Figure 5. Principle of capillary flow porometry.

The Capillary Flow Porometer used in this investigation is shown in Figure 6. It has capability for fully automated test execution, data acquisition, data storage and data reduction. The windows based operation of the instrument is simple. The output of the instrument is reproducible and accurate as demonstrated in Table 1 [4].

Figure 6. The Capillary Flow Porometer used in this study.

Table 1. Comparison of diameters of circular pores measured by SEM and porometry.

		Pore diameter, μm	
Sample	SEM Micrograph	SEM	PMI Porometer
Etched stainless steel disc		81.7 ± 5.2	86.7 ± 4.1
Polycarbonate track etched membrane		4.5 ± 0.5	4.6 ± 0.1

2.3 Liquid Extrusion Porosimetry

For liquid extrusion porosimetry, the sample is placed on a membrane and the pores of the sample and the membrane are spontaneously filled with a wetting liquid (Figure 7A). The membrane is such that its largest pore is smaller than the smallest pore of interest in the sample. Consequently, the gas pressure sufficient to displace liquid from pores of the sample is inadequate to empty the pores of the membrane. Liquid extruded from the pores of the sample under gas pressure flows through the pores of the membrane, while the pores of the membrane remain filled with the liquid and prevent gas from passing through. The differential gas pressure and volume of extruded liquid are measured [5]. For measurement of liquid permeability, the membrane is removed and volume of extruded liquid as a function of differential pressure on excess liquid maintained on the sample is measured (Figure 7B).
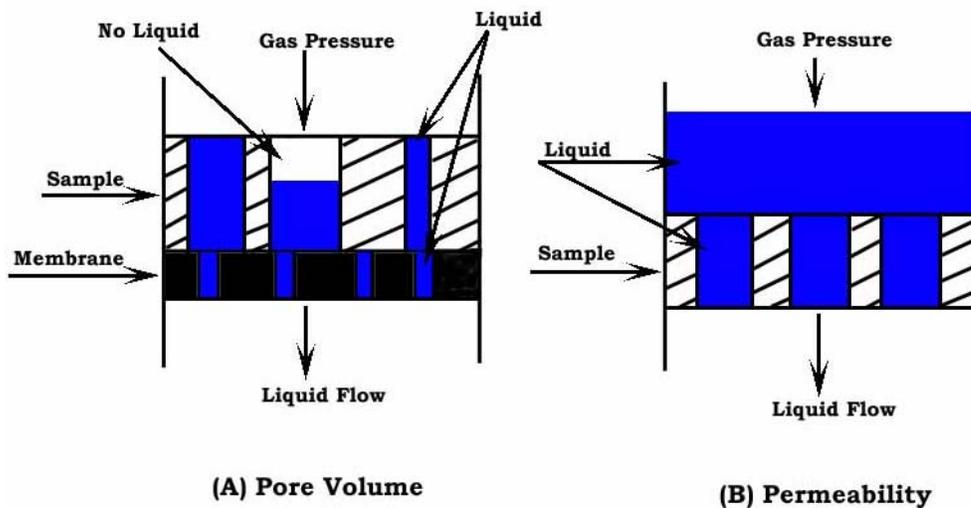
Figure 7: Principle of liquid extrusion porosimetry

The Liquid Extrusion Porosimeter used in this study is shown in Figure 8. It is fully automated. The instrument yields reliable and reproducible data.

Figure 8. The Liquid Extrusion Porosimeter used in this study.

2.4 Mercury intrusion porosimetry

Mercury intrusion porosimetry is a well known technique that has been widely used for pore structure measurement. Mercury is nonwetting to nonwovens because mercury/nonwivven interfacial free energy is greater than that of the gas/nonwoven interface. Mercury does not enter pores spontaneously, but can be forced in to pores. Pressure rerquired to intrude mercury in to a pore is determined by the diameter of the pore. Measure intrusion pressure and intrusion volume yield diameter and volume of through and blind pores. .

3. RESULTS AND DISCUSSION

3.1 Application of capillary flow porometry

Significance of measured pore diameter: Measurements made on a nonwoven using capillary flow porometry are presented in Figure 9. The dry curve represents data obtained with a dry sample and the wet curve corresponds to data from the wet sample. The half-dry curve is not measured. It is calculated from the measured dry curve to yield half of the flow rate through dry sample at a given differential pressure. The use of half-dry curve for the determination of mean flow pore diameter is discussed below. It is shown later that Pore diameter is calculated from differential pressure and a number of other pore characteristics are computed from these data. The pressure required to test nonwovens is usually very low. For the sample used in this study, the pressure required is less than one psi.
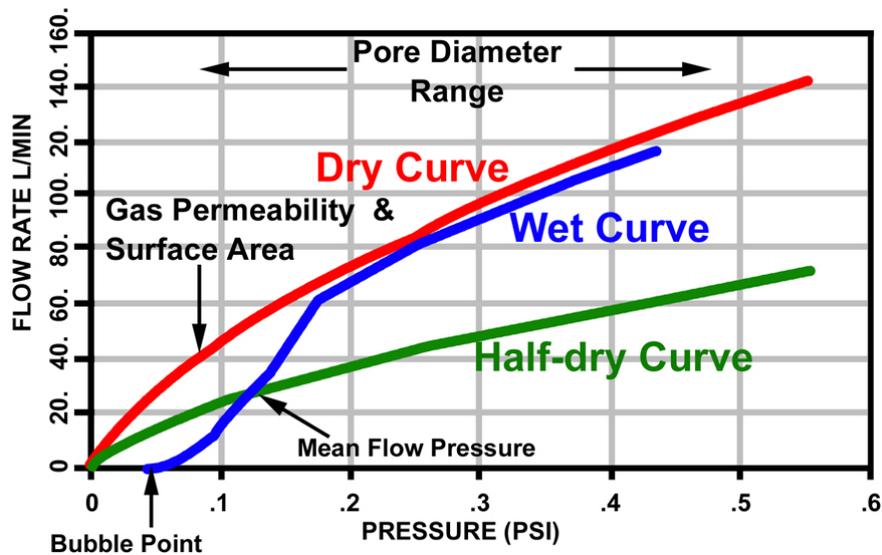

Figure 9: Differential gas pressures and gas flow rates through a sample of nonwoven filter material in wet and dry conditions.

The diameter of a pore normally changes with pore path. In order to understand the diameter that is measured, let us examine the pore in Figure 10. The instrument detects a pore by sensing flow through the pore. Equation 5 suggests that differential pressure required to displace liquid in the pore is inversely proportional to pore diameter. Therefore, pressure required to displace liquid in a pore (Figure 10) would be the highest at the most constricted part of the pore. Once this highest pressure is reached, liquid from the rest of the pore will be removed, gas will start flowing through the pore and the instrument will detect the presence of the pore. Since the measured pressure is the pressure required to displace liquid at the most constricted part of the pore, the calculated pore diameter is the diameter of the pore at its most constricted part. Consequently, all pore diameters measured by extrusion flow porometry are constricted pore diameters.
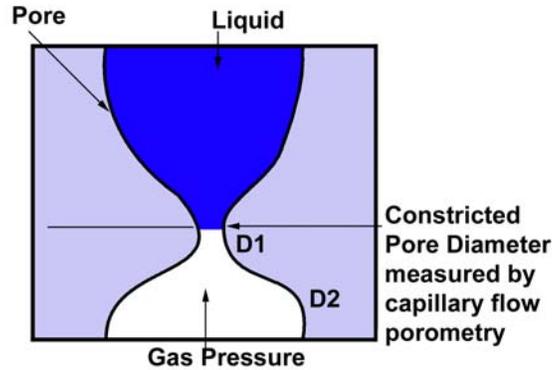
Figure 10: Pore diameter measured by flow porometry.

The largest constricted pore diameter: The largest pore should open up at the lowest pressure. Therefore, the pressure at which flow starts through the wet sample (bubble point) is accurately determined and the pore diameter calculated from this pressure is the largest constricted pore diameter of all pores. The data in Figure 9 yields a value of 149.18 μm. The largest pore diameter gives the smallest particle that can be separated.

The constricted mean flow pore diameter: The mean flow pore diameter is such that fifty percent of flow is through pores larger than the mean flow pore diameter and the rest of the flow is through smaller pores. The mean flow pore diameter is obtained from the mean flow pressure corresponding to the intersection of wet curve and half- dry curve. The data in Figure 9 yield a value of 56.162 μm. Mean flow pore diameter is normally a measure of the size of majority of pores and fluid permeability [6]

Constricted pore diameter range: The bubble point prressure and the pressure at which the dry and wet curves meet yield the pore diameter range. The pore diameter range determines the barrier and flow properties of the nonwoven.

Relation between measured pore diameter and actual pore size: Many pore cross-sections may be considered to be elliptical with minor axis, d, and major axis, nd, as defined in Table 2. Simply by assigning different numbers to n, a variety of pore cross-sections may be generated. For a pore with elliptical cross-section:

$$[dS/dV] \;=\; [1/d]\,[8(1+n^2)/n^2]^{1/2} \tag{6}$$

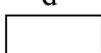Measured pore diameter, D after Equations 4 and 6 becomes:

$$D = \; 4d \,/\, [8(1+n^2)/n^2]^{1/2} \tag{7}$$

The largest particle that can pass through the elliptical pore is d. The ratio of the largest particle that can pass through, d, and the measured pore diameter, D, is defined as the shape factor, λ:

$$\lambda = [d/D] = [(1+n^2) / 2\, n^2]^{1/2} \qquad (8)$$

Values of the shape factor, [d/D], for a few cross-sections are listed in Table 2.

Table 2. Relation between measured and actual pore sizes

Pore cross-section		Shape factor λ (d = λ D)
Circular: n =1	d ○	1
Elliptical: n = 5.	d ⬭ 5d	0.72
Slit: n = 10	d ⬭ 10d	0.71
Square:	d ▢ d	1
Rectangular	d ▭ 2d	0.75

Flow distribution over pore diameter: The pore distribution is presented in Figure 11 as the distribution function, f:

$$f = -\,d\,(F_w / F_d) \times 100) / dD \qquad (9)$$

where F_w and F_d are flow rates through wet and dry samples respectively at the same differential pressure. The distribution function is such that area under the curve (Figure 11) in a pore diameter range is the percentage flow through pores in that range. The distribution shows that the material has a narrow bimodal distribution. Although the pores are in the range of about 20 to 150 μm, most of the pores are in the range of only about 30 to 80 μm and the rest of the pores are negligible. It has been shown that this distribution is close to the pore fraction distribution [7].
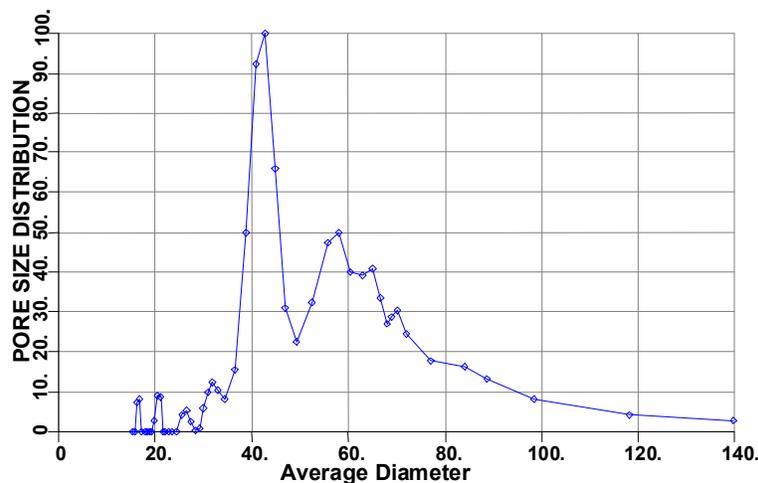

Figure 11: Pore distribution obtained from data in Figure 9.

Gas Permeability: The dry curve gives gas flow rate through dry sample as a function of pressure. Gas permeability in any unit such as Darcy, Frazier, Gurley and Rayle is obtainable at any desired pressure from flow rates of any non-reacting gas measured as a function of pressure.

Liquid permeability: For measurement of liquid permeability, pressure is applied on excess liquid maintained on the sample and the volume of liquid flowing through the sample is measured in a penetrometer attached to the sample chamber. Permeability of liquids including strong chemicals at high pressures and elevated temperatures are measurable [8]. An example is shown in Figure 12.
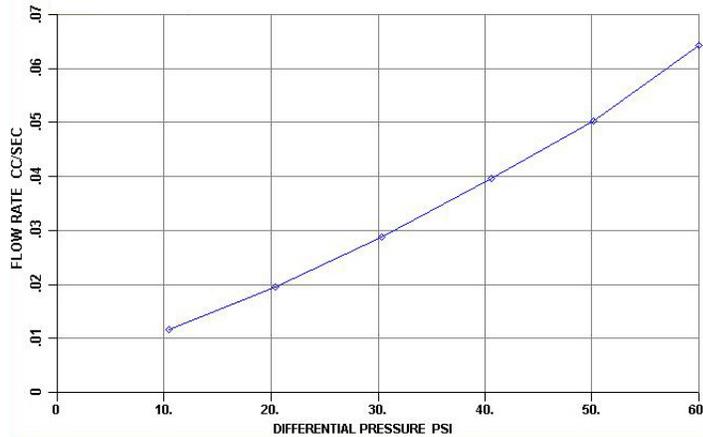

Figure 12. Liquid flow rate of 31% KOH solution through a nonwoven.battery separator material

Envelope (through pore) surface area: Envelope surface area is the surface area of through pores. It is computed from flow rate using the Kozeny- Carman relation between flow rate and surface area [9]. This technique gives accurate values when the surface area is less than about ten m²/g and the pore diameters are not widely different from each other. Typical results are shown in Figure 13. The surface area measured by this technique agrees well with that determined by the gas adsorption technique (Table 3).
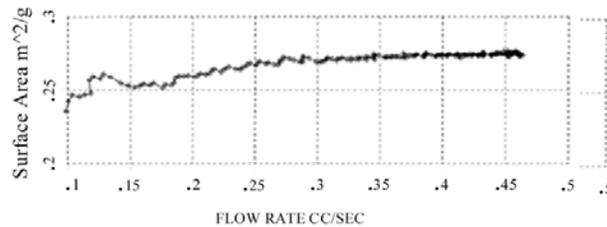

Figure 13. Surface area of a fibrous mat measured as a function of flow rate.

Table 3: Surface area from two techniques.

Technique	Surface area
Porometer	0.56 m²/g
Gas adsorption	0.52 m²/g

Effects of application environment: This technique can also be used to measure the influence of compressive stress [10], cyclic compression [11], temperature, pressure, chemical environment [8], sample orientation [12] and layered structures on pore characteristics. The pore characteristics of individual layers of a composite material can be determined in-situ without separating the materials [13].

3.2 Application of Liquid Extrusion Porosimetry

Pore volume: The cumulative volume of through pores in the nonwoven measured as a function of differential pressure is shown in Figure 14. The pore volume of the nonwoven is 2.4807 cm^3/g. The porosity is 76.78 %. The used pressures given at the top of the figure are less than two psi.
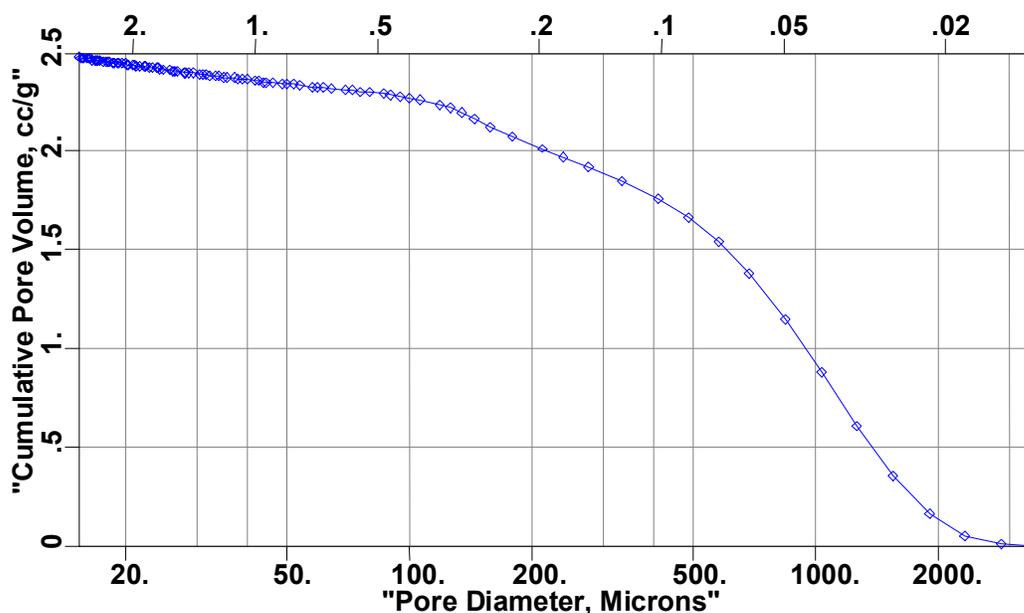

Figure 14. Pore volume measured as a function of pressure

Measured pore diameter & its significance: To understand the measured pore diameters, let us reexamine the same pore (Figure 10) that we investigated earlier. In this technique, the pore diameter and volume of each part of the pore are measured. Because pore diameter is inversely proportional to pressure, pressure required to displace liquid will be the lowest at the wide mouth of the pore (Figure 15). With increasing pressure diameters of narrower parts of the pore and the corresponding pore volumes will be detected. The highest pressure will be required to displace liquid at the most constricted part of the pore (Figure 15). At this highest pressure all the liquid in the rest of the pores will be removed. Therefore, pore volume associated with the highest pressure (the most constricted pore diameter) is the volume of the pore beyond the most constricted part of the pore. Thus, each pore is detected as a set of pores having a range of pore diameters. Measured pore volume as a function of diameter for the pore in Figure 10 is shown in Figure 15.
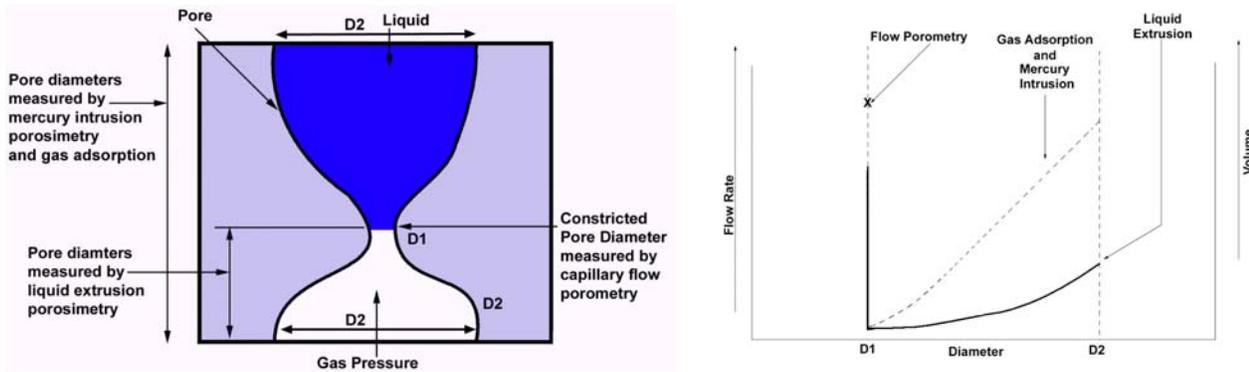
Figure 15: Pore diameter measured by extrusion porosimetry.and other techmiques.

Pore volume distribution over diameter: The pore volume distribution is presented in Figure 16 as the distribution function, f_v:

$$f_v = - [d \, V / d \log D] \qquad\qquad (10)$$

where V is the pore volume**.** The distribution function is such that area under the curve (Figure 16) in a pore diameter range is the volume of pores in that range. The distribution shows that the material has a broad distribution. Although the large pore openings are as much as about 2 mm, most pores are in the range of about 2000 to 50 μm and the rest of the pores are negligible.
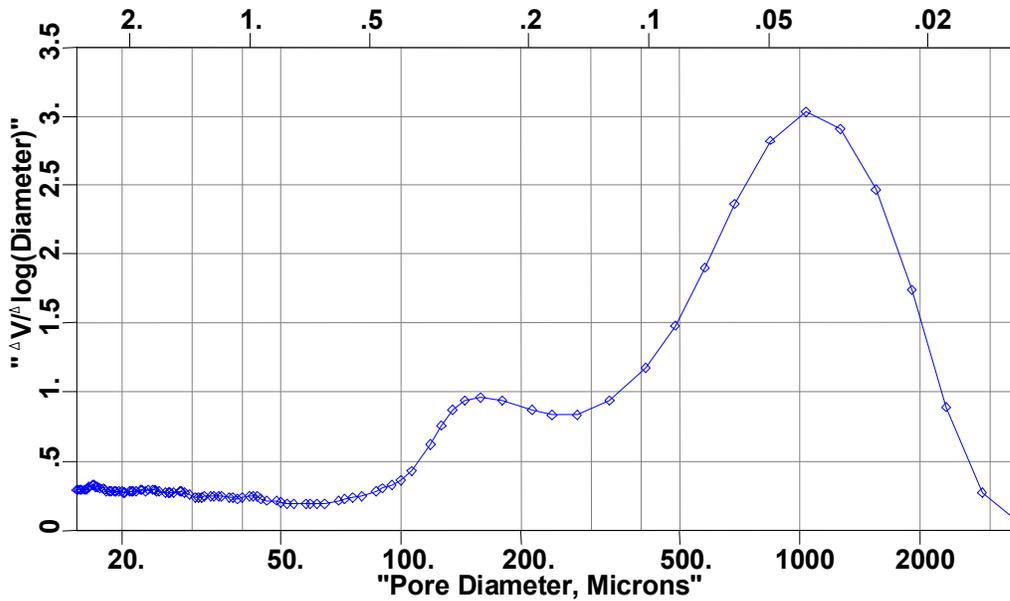

Figure 16: Pore volume distribution

Converging or diverging pores: One interesting characteristic of this technique is that converging or diverging nature of the pore shape can be detected. After completion of a test, the test is repeated with the sample turned upside down. From the two distribution functions, the pore shape orientation is inferred. This is schematically illustrated in Figure 17. No other test has such capability.
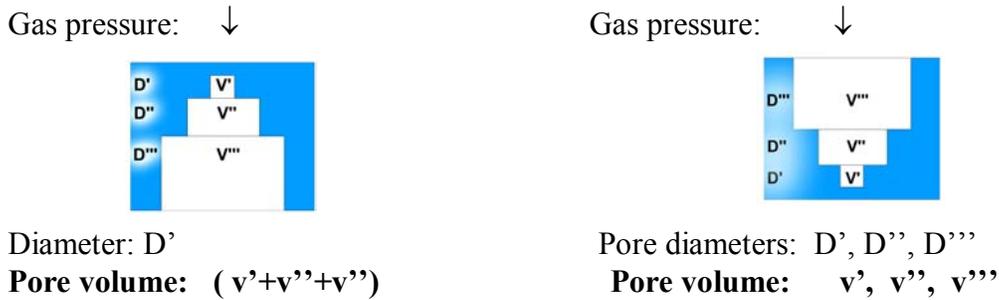
Gas pressure: ↓   Gas pressure: ↓

Diameter: D'   Pore diameters: D', D'', D'''

Pore volume: (v'+v''+v'')   **Pore volume: v', v'', v'''**

Figure 17. Determination of converging or diverging nature of the pore.

Envelope (through pore) surface area: Integration of Equation 3 shows that:

$$S = [1/(\gamma \cos \theta)] \int pdV \tag{11}$$

This relation is used to obtain surface area of through pores from volume measured as a function of pore diameters. The data in Figure 14 yield a value of 0.043 m^2/g.

Liquid permeability: Liquid permeability is obtained by measuring the volume of liquid flow due to differential pressure applied on excess liquid maintained on the sample. If the permeability of the membrane is comparable or less than that of the sample, the membrane is removed before performing the liquid permeability test.

3.3 Application of mercury intrusion porosimetry

Mercury intrusion porosimetry measures cumulative4 pore volume as a function of pore diameter. The results obtained with a nonwoven is presented in Figure 18. The pore volume distribution in terms of the distribution function in Equation 10 is shown in Figurer 19.The stregth of the technique is that it measures the pore volume and all the diameters (Figure 15) of through and blind pores (Figure 1) and almost any nonwiven can be tested. However, the technique requires use of a toxic material and cannot measure any of the flow properties. The techniques will be compared in the following section.
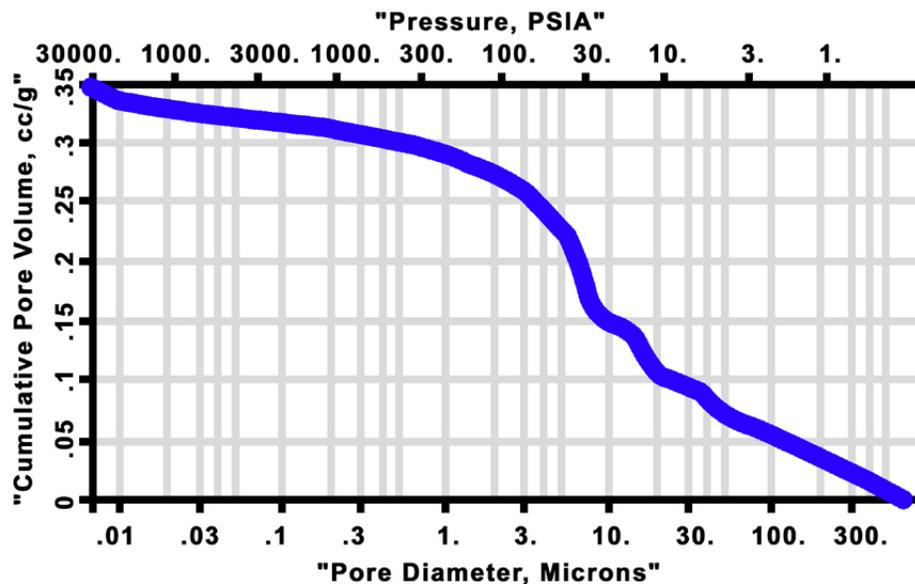

Figure 18 Cumulative pore volume determined as a function of pore diameter in a battery separator by mercury intrusion porosimetry.
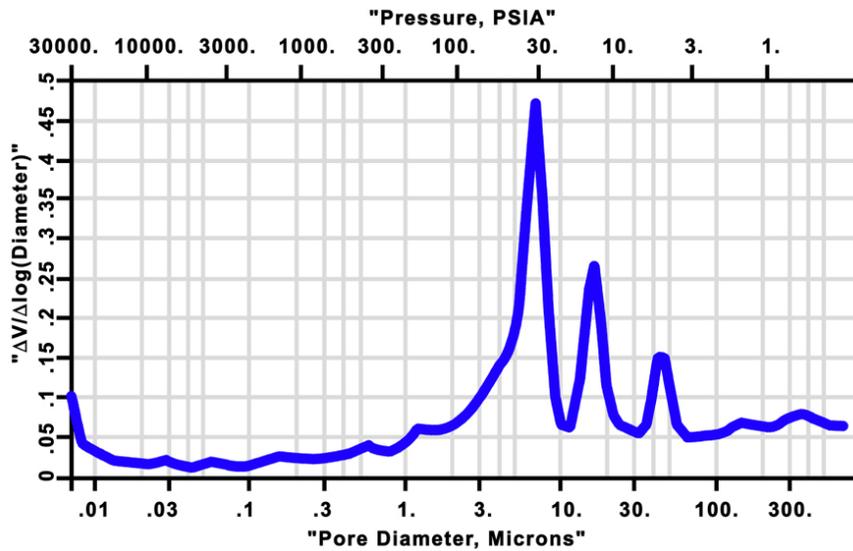
Figure 19. Pore volume distribution. Area under the curve in a given pore size range is the volume of pores in that range.

3.4 Strengths and limitations of the techniques

The strengths and limitations of the two liquid extrusion methods are considered in Table 4. For comparison, the characteristics of the mercury intrusion technique, which is often used for pore structure characterization are included.

4 SUMMARY AND CONCLUSION

1. The extrusion techniques, flow porometry and extrusion porosimetry, for pore structure characterization have been discussed.
2. Results obtained using the two extrusion techniques have been presented to illustrate the application of these techniques.
3. The results have been analyzed and interpreted.
4. A comparison of the characteristics of the two techniques as well as the mercury intrusion technique has been presented.
5. Recent developments in the extrusion techniques for pore structure analysis of nonwovens permit accurate determination of a very wide variety of properties.
6. Extrusion techniques are quite versatile, do not use any toxic material and are capable of wide application.

Table 4: Characteristics of different techniques

Characteristics	Extrusion (Capillary Flow) Porometry	Extrusion Porosimetry	Intrusion Porosimetry
Pore diameter			
Diameter at most constricted part	Yes	No	No
Largest constricted Pore diameter	Yes	No	No
Mean constricted pore diameter	Yes	No	No
Many diameters of a pore	No	Yes	Yes
Median diameter based on volume	No	Yes	Yes
Pore volume			
Through pore	No	Yes	No
Through & blind pore	No	No	Yes
Distribution	No	Yes	Yes
Pore shape			
Through pore	Yes	Yes	No
Through & blind pore	No	No	Yes
Converging/diverging pores	No	Yes	No
Surface area			
Through pore	Yes	Yes	No
Through & blind pore	No	No	Yes
Permeability			
Liquid	Yes	Yes	No
Gas	Yes	No	No
Effects of Service conditions			
Compressive stress	Yes	Yes	No
Stress cycles	Yes	Yes	No
Temperature	Yes	Yes	No
Strong chemical environment	Yes	Yes	No
Orientation	Yes	No	No
Graded/multiple layer structure	Yes	No	No
Operational features			
Non-toxic material	Yes	Yes	No
Low pressure	Yes	Yes	No

References

1. K. Denbigh, The Principles of Chemical Equilibrium, Cambridge Equilibrium, 1968.
2. A. K. Jena and K. M. Gupta, 'In-plane compression porometry of Battery separators', Journal of Power Sources, 1999, vol.80, p. 46.
3. A. W. Adamson, 'Physical Chemistry of Surfaces' Interscience, 1967.
4. Akshaya Jena and Krishna Gupta, 'Characterization of Pore Structure of Filter Media', Fluid/Particle Separation Journal, 2002, vol. 14, No. 3, p. 1.
5. Akshaya Jena and Krishna Gupta, 'Measurement of Pore Volume and Flow through Porous Materials'.MP Material Prufung', 2002, Jahrg. 44, p. 243.
6. Mayer
7. A. K. Jena and K. M. Gupta, 'Pore size Distribution in Filter Materials', Book of Papers, FILTRATION 99, International Conference, Association of the Nonwoven Fabric Industry, 1999, p.24.0.
8. Akshaya Jena and Krishna Gupta, 'Evaluation of Permeability of Strong Chemicals at Elevated Temperatures and High Pressures', The 2002 17th Annual Battery Conference on Applications and Advances, California State University, Long Beach, California, Proceedings/December 2001, IEEE Catalog Number 02TH8576.
9. Gerard Kraus, J.W. Ross and L. A. Girifalco, 'Surface Area Analysis by Means of Gas Flow Methods: I Steady State Flow in Porous Media, Phys. Chem., 1953, vol. 57, p. 330.
10. Vibhor Gupta and A.K. Jena. 'Effects of Compression on Porosity of Filter Materials'. Advances in Filtration and Separation Technology, The American Filtration and Separation Society, Northport, Alabama, 1999, Vol. 13a, p.10.
11. Akshaya Jena and Krishna Gupta, 'Effects of Cyclic Compression on Pore Structure of Battery Materials', Proceedings of the 19th International Seminar and Exhibition on Primary and Secondary Batteries, March, 11-14. 2002, Fort Lauderdale, Florida.
12. Akshaya Jena and Krishna Gupta, 'In-Plane and Through-Plane Porosity in Coated Textile Materials', Journal of Industrial Textiles', 2000, vol. 29, Number 4, April, p.317.
13. A. Jena and K. Gupta, 'Analyse der Porendurchmesser von Mehrschichtfiltermitteln', F&S Filtrieren und Separieren, 2002, Jahrg. 16, 2002, Nr. 1, p.13.